

## Capability of three-dimensional speckle tracking radial strain for identification of patients with cardiac sarcoidosis

Takayuki Tsuji · Hidekazu Tanaka · Kensuke Matsumoto · Tatsuya Miyoshi · Mana Hiraishi · Akihiro Kaneko · Keiko Ryo · Yuko Fukuda · Kazuhiro Tatsumi · Tetsuuri Onishi · Hiroya Kawai · Ken-ich Hirata

Received: 10 May 2012 / Accepted: 21 July 2012 / Published online: 1 August 2012  
© Springer Science+Business Media, B.V. 2012

**Abstract** Since cardiac sarcoidosis (CS) leads to substantial morbidity and sudden death, early diagnosis and appropriate management are crucial for patients with CS. Echocardiography used to be considered a useful diagnostic tool for patients with CS, but CS may clinically present as dilated cardiomyopathy (DCM). Our objective was to investigate whether a novel three-dimensional (3-D) speckle-tracking strain can identify patients with CS more accurately. We studied 23 CS patients with an ejection fraction (EF) of  $46 \pm 10\%$ , and 16 EF-matched patients with DCM (EF  $45 \pm 11\%$ ). Global radial (GRS), circumferential (GCS) and longitudinal (GLS) strain was assessed using 3-D speckle-tracking system. GRS of patients with CS was significantly lower than that of patients with DCM ( $18.5 \pm 8.4$  vs.  $28.5 \pm 8.3\%$ ,  $p < 0.01$ ), but GCS and GLS in patients with CS and DCM were similar.  $GRS \leq 21.1$  could differentiate CS from DCM with a sensitivity of 70 %, specificity of 88 % and area under the curve of 0.79. An additional noteworthy findings was that, patients with CS showed more negative radial strain curves than did those with DCM ( $1.7 \pm 2.3$  vs.  $0.1 \pm 0.5$ ,  $p < 0.01$ ). In conclusion, 3-D speckle-tracking radial strain shows good potential to distinguish CS from DCM. Our observations can thus be expected to have clinical implications for management of CS patients.

**Keywords** Cardiac sarcoidosis · Echocardiography · Heart failure · Speckle-tracking strain · Ventricular function

### Introduction

Sarcoidosis is a systemic granulomatous disease of undefined cause involving multiple organs [1]. Although its cardiac involvement has been demonstrated in 20–50 % of sarcoidosis patients in autopsy studies, clinical cardiac manifestations have been seen in only about 5 % [1, 2]. Cardiac sarcoidosis (CS) entails significant morbidity and mortality due to fatal arrhythmia, atrioventricular conduction disturbance, and refractory congestive heart failure, but its diagnosis has not always been easy. Furthermore, steroid therapy may be protective or therapeutic for preventing left ventricular (LV) remodeling and preserving LV function in the early or middle stage of CS, but it may not be as effective in the late stage [3]. Early diagnosis and appropriate management for patients with CS are thus essential.

Echocardiography used to be considered a useful diagnostic tool for patients with CS, but CS may clinically present as dilated cardiomyopathy (DCM). Furthermore, a previous study of cardiac transplant found that 83 % of CS patients had been misdiagnosed in pre-transplantation investigations [4]. A newly developed three-dimensional (3-D) speckle-tracking strain, which uses complete 3-D pyramidal datasets, has provided a new insight into LV mechanics [5–8]. The potential advantages of such a system are the ability to express myocardial function of the whole heart, independence of tomographic imaging planes, and the ability to analyze regional ventricular function by using 3 different strains from the same heart beat acquisition. The

T. Tsuji · H. Tanaka (✉) · K. Matsumoto · T. Miyoshi · M. Hiraishi · A. Kaneko · K. Ryo · Y. Fukuda · K. Tatsumi · T. Onishi · H. Kawai · K. Hirata  
Division of Cardiovascular Medicine, Department of Internal Medicine, Kobe University Graduate School of Medicine, 7-5-2, Kusunoki-cho, Chuo-ku, Kobe 650-0017, Japan  
e-mail: tanakah@med.kobe-u.ac.jp

3-D speckle-tracking strain imaging system was thus found to be more effective for quantification of LV performance than was previously possible with two-dimensional (2-D) methods. The objective of our study was therefore to test the hypothesis that novel 3-D speckle-tracking strain can identify patients with CS more accurately.

## Methods

### Study population

The study group consisted of 26 consecutive patients with CS and LV dysfunction. Three patients with suboptimal echocardiographic images were excluded from all subsequent analyses. The eventual patient study group thus consisted of 23 CS patients, 11 (48 %) of whom were female (Table 1). The group's mean age was  $64 \pm 12$  years and mean ejection fraction (EF) was  $46 \pm 10$  %. CS was diagnosed according to the guidelines of the Japan Ministry of Health and Welfare [9]. For baseline comparison, we also studied 16 EF-matched DCM patients with (mean age:  $59 \pm 11$  years; EF:  $45 \pm 11$  %). The diagnosis of DCM was established with the following criteria: (1) presence of LV dilation; (2) reduced LV ejection fraction; (3) coronary angiographic evidence of absence of coronary artery disease defined as  $>50$  % stenosis of a major epicardial vessel or a history of myocardial infarction (4) absence of primary valvular heart disease; (5) absence of cardiac muscle disease secondary to any known systemic diseases. The diagnosis of DCM was supported by endomyocardial biopsy findings. At the time of enrolment, all patients with CS and DCM were sinus rhythm, and in clinically stable condition and on optimal and maximally tolerated pharmacological therapy. This study was approved by the local ethics committee of our institution, and written informed consent was obtained from all patients.

### Echocardiographic examination

All echocardiographic studies were performed with a commercially available echocardiography system (Aplio Artida; Toshiba Medical Systems, Tochigi, Japan). Digital routine greyscale 2-D cine loops from three consecutive beats were obtained at end expiratory apnea from the standard apical views, parasternal long-axis view, and mid-LV short-axis views at depths of 11–20 cm (mean:  $16 \pm 2$  cm). Frame rates were 44–90 Hz (mean  $59 \pm 11$  Hz) for greyscale imaging. Sector width was optimized to allow for complete myocardial visualization while maximizing the frame rate. LV dimensions were calculated from the standard M-mode images obtained at the parasternal long-axis views and included LV diameters and end-diastolic thickness of the

interventricular septum and posterior wall. The pulsed-wave Doppler derived transmitral velocity and digital color tissue Doppler derived mitral annular velocity were obtained from the apical 4-chamber view for assessment of diastolic function. Early diastolic (E), atrial (A) wave velocities, E/A ratio, and E wave deceleration time were measured with the aid of pulsed-wave Doppler recording. Spectral pulsed wave Doppler derived early diastolic velocity (E') was obtained from the septal mitral annulus, and E/E' was calculated for an estimate of LV filling pressure.

### 3-D speckle-tracking data acquisition

All 3-D echocardiographic studies were performed with a 2.5-MHz 3-D matrix array transducer (Toshiba Medical Systems, Tochigi, Japan). Digital data were transferred to dedicated software (Ultra Extend, Toshiba Medical Systems, Tochigi, Japan) for all subsequent analyses. 3-D speckle-tracking analysis was performed as previously described in detail [5, 7, 8]. Briefly, 3-D speckle-tracking used a pyramidal volume from the matrix array transducer. Acquisition of a full-volume dataset required the acquisition of smaller wedge-shaped subvolumes from 4 or 6 consecutive cardiac cycles obtained during a single breath hold, which were then combined to provide the larger pyramidal volume. The mean volume rate was  $22 \pm 2$  volumes/s for gray scale imaging used for 3-D speckle-tracking analysis. The 3-D datasets were displayed in 5 different cross sections comprising the 3 standard short-axis views and the apical 4- and 2-chamber views that could be modified interactively. The apical views were used for the placement of regions of interest on the endocardium and epicardium and the endocardium and epicardium were retraced as necessary to achieve suitable tracking. These contours were then used to obtain LV end-diastolic and end-systolic volumes from the LV volume curves as the respective maximum and minimum values. LV ejection fraction (LVEF) could be obtained automatically [5]. Radial, circumferential and longitudinal myocardial functions were quantified as global peak strains by using 3-D speckle-tracking strain imaging from all 16 LV segments (Fig. 1).

### Statistical analysis

Continuous variables are expressed as mean values  $\pm$  SD or percentages, while categorical data are summarized as frequencies and percentages. The unpaired *t* test or  $\chi^2$  test was used for comparing parameters of groups, and proportional differences were evaluated by using Fisher's exact test or  $\chi^2$  test as appropriate. The diagnostic performance of 3-D speckle-tracking strain parameters used for differentiating patients with CS from those with DCM was evaluated by means of receiver operating characteristic curve

**Table 1** Clinical and Hemodynamic characteristics of patients

	Patients with CS (n = 23)	Patients with DCM (n = 16)	p value
Age (years)	64 ± 12	59 ± 11	0.21
Gender (M/F)	12/11	11/5	0.31
Hemodynamics			
Systolic blood pressure (mmHg)	110 ± 14	115 ± 15	0.31
Diastolic blood pressure (mmHg)	61 ± 9	66 ± 9	0.07
Heart rate (bpm)	63 ± 9	68 ± 7	0.06
QRS duration (ms)	117 ± 29	109 ± 24	0.06
Abnormal electrocardiogram			
Atrioventricular block (n (%))	8 (35)		
Left bundle brunch block (n (%))	1 (4)		
Right bundle brunch block (n (%))	4 (17)		
Non-sustained ventricular tachycardia (n (%))	11 (48)		
Sustained ventricular tachycardia (n (%))	7 (30)		
NYHA functional class (n (%))			
I	17 (74)	10 (63)	0.73
II	6 (26)	6 (37)	0.46
III	0 (0)	0 (0)	
IV	0 (0)	0 (0)	
Medication			
Loop diuretics (n (%))	7 (30)	6 (38)	0.46
β blockers (n (%))	13 (57)	15 (94)	0.01
Spironolactone (n (%))	4 (17)	6 (38)	0.17
ACE-I/ARBs (n (%))	16 (70)	15 (94)	0.07
Steroid (n (%))	7 (30)		
Patients with myocardial biopsy (n (%))	16 (70)		
Patients with myocardial positive biopsy results (n (%))	3 (13)		
Extracardiac sarcoidosis			
Lung (n (%))	8 (35)		
Lymph node (n (%))	5 (22)		
Skin (n (%))	3 (13)		
Liver (n (%))	0 (0)		
Eye (n (%))	4 (17)		
Other (n (%))	1 (4)		
Serum ACE level (IU/l)	9.9 ± 5.1		
Exercise tolerance data			
Peak VO <sub>2</sub> (ml/kg/min)	15.4 ± 3.1		
VE/VCO <sub>2</sub> slope	24.1 ± 3.2		
Patients undergoing CMR (n (%))	13 (57)		
Late gadolinium enhanced CMR, n (%)	13 (100)		

Data are presented as *n*, mean ± SD or *n* (%). The serum ACE level and exercise tolerance data were assessed in a subset of 16 and 8 CS patients, respectively

CS cardiac sarcoidosis, DCM dilated cardiomyopathy, NYHA New York Heart Association, ACE-I angiotensin converting enzyme-inhibitor, ARB angiotensin II receptor blocker, VO<sub>2</sub> oxygen consumption, VE ventilation, VCO<sub>2</sub> carbon dioxide production, CMR cardiac magnetic resonance

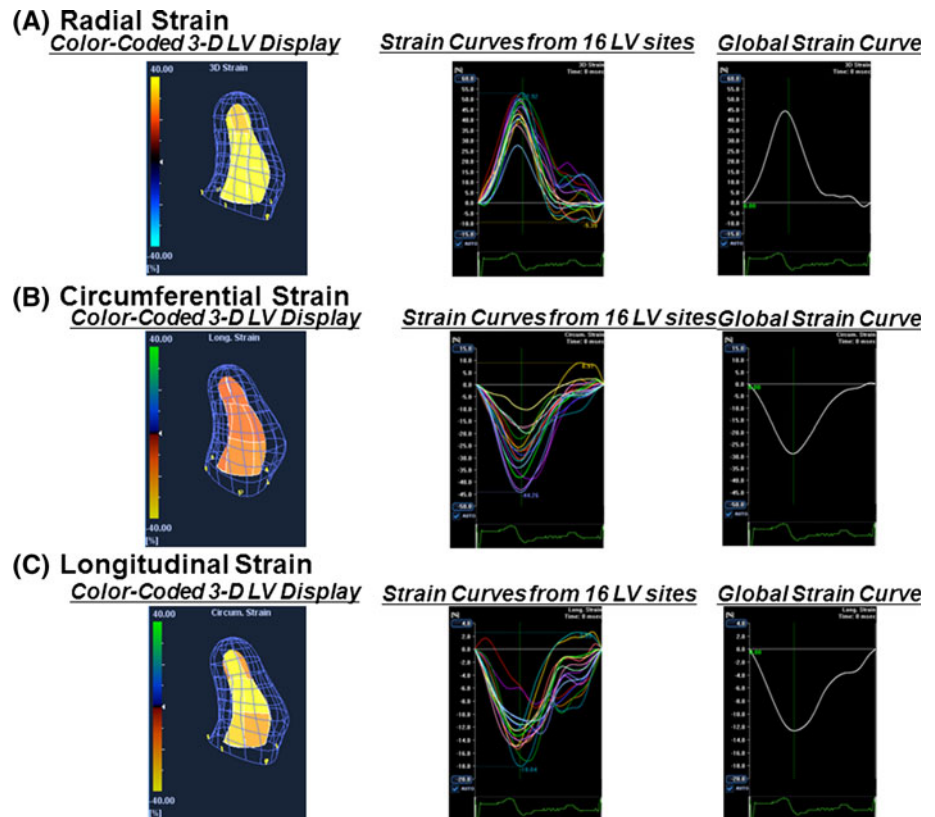
analysis. The intraclass correlation coefficient was used to determine inter- and intra-observer reproducibility for 3-D speckle-tracking strain from 20 randomly selected subjects. For all steps, *p* value of <0.05 was considered statistically significant. All the analyses were performed with commercially available software (MedCalc software version 10.4.0.0, MedCalc Software, Inc., Mariakerke, Belgium).

## Results

### Baseline characteristics

The baseline clinical and hemodynamic characteristics of the 23 patients with CS and the 16 EF-matched patients with DCM are summarized in Table 1. Age, gender

**Fig. 1** An example of color-coded 3-dimensional (3-D) left ventricular (LV) display (left), corresponding time-to-strain curves from 16 LV sites (middle) and global strain curve (right) for longitudinal (a), radial (b), and circumferential (c) speckle-tracking strain imaging. Each dyssynchrony was quantified as standard deviation for the time-to-peak strain by using each of the 3-D speckle-tracking strains from all 16 LV segments. Furthermore, each myocardial function was quantified as a global peak strain by using the 3-D speckle-tracking strains from all 16 LV segments



distribution, blood pressure and heart rate of patients with CS were similar to those of patients with DCM.

Comparison of conventional echocardiographic parameters

LV and left atrial diameters and end-diastolic thickness of the interventricular septum and posterior wall were similar for patients with CS and DCM. Global diastolic function including E/A ratio and E/E' was also similar for the 2 groups.

Comparison of 3-D peak global strain

GCS and GLS in patients with CS and DCM were similar, but GRS in patients with CS was significantly lower than that in patients with DCM ( $18.5 \pm 8.4$  vs.  $28.5 \pm 8.3$  %,  $p < 0.01$ ; Fig. 2). An important finding was that the receiver operating characteristic curve analysis identified  $GRS \leq 21$  as the best predictor for differentiating CS from DCM with a sensitivity of 70 %, specificity of 88 %, and area under the curve of 0.793 (95 % CI 0.639–0.906;  $p < 0.001$ ; Fig. 3). Furthermore, patients with CS showed a higher number of negative radial strain curves than did those with DCM ( $1.7 \pm 2.2$  % vs.  $0.1 \pm 1.0$  %,  $p < 0.01$ , Fig. 4). Figure 5 shows representative examples of GRS, GCS and GLS from a patient with CS and DCM (Table 2).

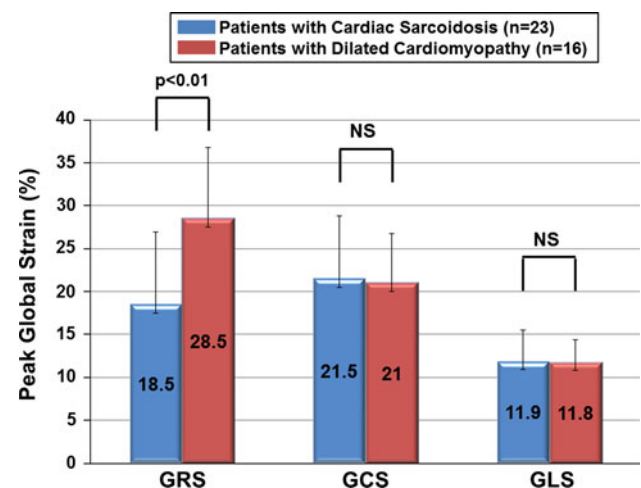


**Fig. 2** Comparison of three-dimensional speckle-tracking strain for patients with cardiac sarcoidosis (CS) and dilated cardiomyopathy (DCM), demonstrating that global circumferential (GCS) and longitudinal strain (GLS) for patients with CS and DCM were similar, but that global radial strain (GRS) for patients with CS was significantly lower than that for patients with DCM

Reproducibility

The intraclass correlation coefficients for inter-observer reproducibility of global 3-D speckle-tracking peak strain were 0.957 (95 % CI, 0.826–0.989) for radial, 0.916 (95 % CI, 0.663–0.979) for circumferential, and 0.958 (95 % CI,

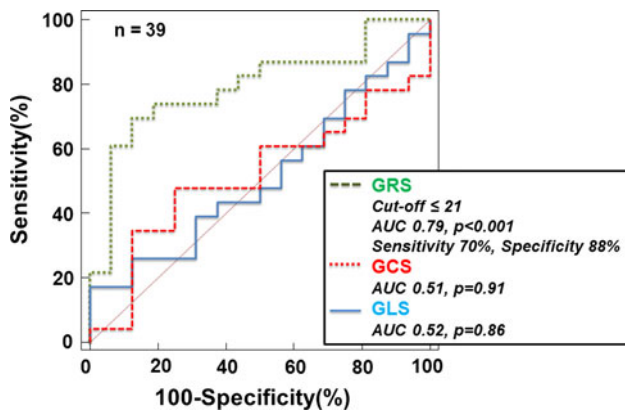


**Fig. 3** Receiver operating characteristic curve analysis identified  $GRS \leq 21$  as the best predictor for differentiating CS from DCM. Abbreviations are the same as in Fig. 2

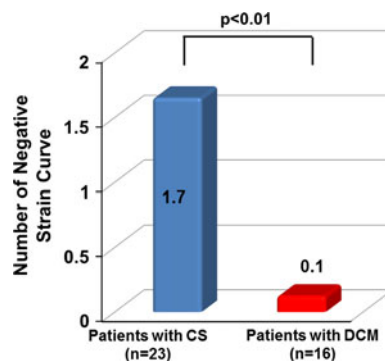


**Fig. 4** Number of negative radial strain curves for patients with CS and DCM, demonstrating that patients with CS showed a higher number of negative radial strain curves than did those with DCM. Abbreviations are the same as in Fig. 2

0.831–0.990) for longitudinal strain, while the corresponding coefficients for intra-observer reproducibility were 0.926 (95 % CI, 0.703–0.982), 0.914 (95 % CI, 0.655–0.979), and 0.977 (95 % CI, 0.908–0.994).

## Discussion

The study reported here is the first to demonstrate the efficacy of 3-D speckle-tracking radial strain for identifying patients with CS. GRS in patients with CS was significantly lower than that in patients with DCM. On the other hand, GCS and GLS in patients with CS and DCM were similar. Noteworthy was that,  $GRS \leq 21$  could differentiate patients with CS from those with DCM. Furthermore, patients with CS showed a higher number of negative radial strain curves than those with DCM. These findings suggest the non-uniformity of cardiomyocyte damage in patients with CS, so that 3-D speckle-tracking

radial strain may help differentiate CS patients with relatively mild LV dysfunction from DCM patients.

## Diagnostic test for CS

Because of the potential life-threatening complications of CS and the potential benefit of treatments including steroid therapy, all patients diagnosed with sarcoidosis should be screened for cardiac involvement. Since the clinical manifestations are nonspecific, diagnostic tests such as endomyocardial biopsy or imaging may be required. However, endomyocardial biopsy, a diagnostic tool for evaluating CS, has a low sensitivity of 20 % due to random distribution of granulomas [10], while conventional echocardiographic technique may be nonspecific because the ventricular septum or the LV free wall appears hyperechogenic when there is granulomatous involvement and scar formation [11]. Detection of a thinning anterior septum with increased echogenicity is highly suggestive of but not definitive for CS [12]. A further clue, however is the presence of echocardiographic regional wall motion abnormalities without associated coronary vessel disease. In this study, conventional echocardiographic techniques including global LV systolic and diastolic functions failed to accurately identify patients with CS.

Several investigators reported that cardiac magnetic resonance (CMR) imaging may improve the sensitivity of diagnosis of CS. In addition, late gadolinium enhancement has emerged as the dominant CMR sequence for evaluation of CS and assessment of efficacy of steroid therapy [13–16]. In fact, the extent of late gadolinium enhancement correlates with the risk of sudden cardiac death. More recently, Patel et al. [16] demonstrated that late gadolinium enhancement was useful for defining myocardial damage in patients with sarcoidosis and preserved EF and no known history of CS. Although recent introduction of CMR is compatible for patients with an implantable cardioverter-defibrillator or pacemaker, a majority of CMR in the clinical setting is still contraindicated for such patients, and is also costly. In addition, patients with renal dysfunction would be another issue for contrast CMR, and those with arrhythmias including ectopy or atrial fibrillation might also be a technical difficulty with ECG electrocardiogram-gated CMR. In fact, 10 of the patients in this study (43 %) were unable to undergo CMR due to the presence of an implantable cardioverter-defibrillator or pacemaker.

## 3-D speckle tracking strain for assessment of multidirectional myocardial functions

In this study, we evaluated the 3 different components of myocardial deformation in patients with CS and DCM, and demonstrated that radial strain in patients with CS was

**Fig. 5** Representative case of global radial (GRS, *top*), circumferential (GCS, *middle*), and longitudinal (GLS, *bottom*) strain curves for a patient with cardiac sarcoidosis (CS) and one with dilated cardiomyopathy (DCM). Left ventricular end-diastolic (LVEDV) and end-systolic volume (LVESV), ejection fraction (LVEF), and mitral inflow E and mitral E' annular velocities ratio (E/E') were similar for the two types. On the other hand, GRS for the patient with CS was significantly lower than that for the patient with DCM

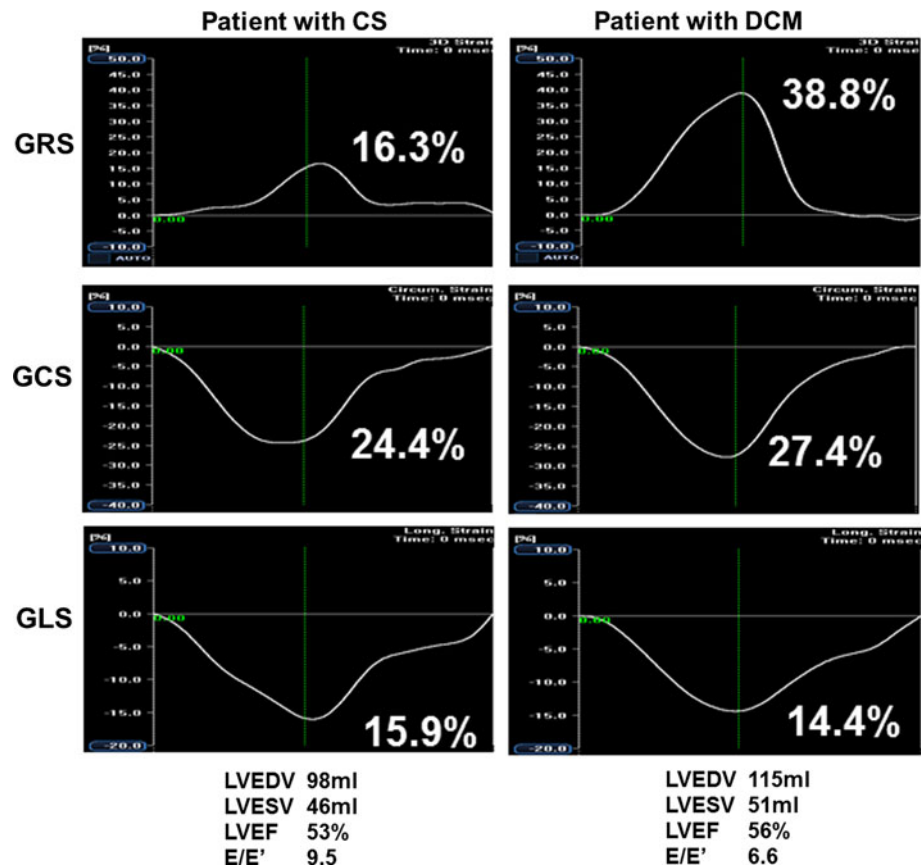


**Table 2** Echocardiographic characteristics of patients

	Patients with CS (n = 23)	Patients with DCM (n = 16)	p value
LV end-diastolic diameter (mm)	52 ± 10.7	55.7 ± 8.1	0.28
LV end-systolic diameter (mm)	39.8 ± 12.8	42.8 ± 10.7	0.45
End-diastolic thickness of the interventricular septum (mm)	9.5 ± 2.7	9.3 ± 2.0	0.79
End-diastolic thickness of the posterior wall (mm)	9.2 ± 1.7	8.8 ± 1.6	0.46
Left atrial diameter (mm)	40.4 ± 6.9	40.3 ± 8.1	0.95
LV end-diastolic volume (ml)	115.6 ± 41.2	133.9 ± 48.7	0.21
LV end-systolic volume (ml)	46.9 ± 36.3	76.7 ± 44.5	0.37
LV ejection fraction (%)	46.4 ± 9.8	45.1 ± 10.6	0.70
E/A ratio	0.82 ± 0.21	0.97 ± 0.33	0.09
E/E' ratio	11.6 ± 4.3	9.4 ± 3.8	0.11
E'	6.2 ± 1.8	7.4 ± 2.7	0.10
GLS	12.2 ± 4.3	11.8 ± 2.6	0.94
GRS	18.5 ± 8.4	28.5 ± 8.3	0.0007
GCS	23.8 ± 7.3	21.0 ± 5.8	0.83

Data are presented as *n*, mean ± SD or *n* (%). *CS* cardiac sarcoidosis, *DCM* dilated cardiomyopathy, *LV* Left ventricular, *A* atrial wave velocity, *E* early diastolic wave velocity, *E'* early diastolic mitral annular velocity. *GLS* global longitudinal strain, *GRS* global radial strain, *GCS* global circumferential strain

significantly lower than that in patients with DCM. LV systolic function is a complex, coordinated action resulting from longitudinal and circumferential contraction. The subepicardial and subendocardial layers are longitudinally oriented and thus make a significant contribution to long-

axis function, whereas the middle layer is circumferentially arranged and contributes to short-axis function. In addition, radial function is associated with wall thickening within the whole myocardium. This non-uniformity of fiber orientation may explain the non-uniform susceptibility of the

various layers to injury. Since LV performance in reality is a 3-D phenomenon, the 2-dimensional speckle-tracking method may oversimplify the complexities of LV function. The novel 3-D speckle-tracking system, on the other hand, can quantify 3 different strains simultaneously from all 16 LV segments. Since the 3-D speckle-tracking system used in our study could provide a comprehensive evaluation of true global strain from complete 3-D data sets, it could yield more accurate information than was previously possible with the 2-D system. Our study found that only radial strain was lower for patients with CS than in those with DCM, but circumferential and longitudinal strains were similar in both groups. In this 3-D speckle-tracking strain method, radial strain is estimated by both endocardial and epicardial speckle-tracking strain, whereas circumferential and longitudinal strain are estimated by endocardial speckle-tracking strain [17]. However, it remains unknown regarding which is more predominant in the endocardial, middle or epicardial portion of the LV wall for estimation of radial strain. Sarcoid infiltration often occurs in the middle or epicardial portion of the LV wall in the early stage [18, 19], thus our findings may be reflected by such phenomenon in CS patients with relatively mild LV dysfunction. There were any autopsy or CMR data to support more epicardial distribution of the granulomas to support our findings on why GRS was a good differentiating tool. Of 23 CS patients, a subset of 13 patients performed CMR in this study. 5 patients were revealed with late enhancement in the epicardial portion, 3 in the middle portion, 1 were in the endocardial portion, and 4 were in the transmural myocardium. There were no statistically differences for the distribution of CMR with late enhancement. Based on our findings, we believe that GRS by means of 3-D speckle-tracking method could be a sensitive parameter, and has ability for predicting early subtle changes by sarcoid infiltration compared to CMR with late enhancement.

#### Clinical implications

The long-term benefits of steroid therapy for reducing clinical morbidity and mortality have been demonstrated for patients with CS. Furthermore, previous investigators have reported that steroid therapy for sarcoidosis is more effective for the heart than for other organs [20, 21]. Based on the poor prognosis of CS and the relatively high prevalence of sudden cardiac death, recent guidelines have asserted that implantable cardioverter-defibrillators implantation is a reasonable therapeutic procedure for patients with CS (Class IIa), thus making identification of patients with CS clinically important, and early diagnosis and appropriate treatment crucial. Various imaging modalities, especially echocardiography, used to be considered effective diagnostic tools for patients with CS, but CS may clinically present as DCM so that

patients with CS may be misdiagnosed as DCM. As a result, CS continues to remain a challenging diagnostic and management entity. 3-D speckle-tracking radial strain, however, appears to have potential for differentiating CS from DCM among patients with relatively mild LV dysfunction (EF 45–50 %), and thus help provide early diagnosis and appropriate management for such patients. Furthermore, 3-D speckle-tracking method may be applied for the diagnosis of other cardiomyopathies.

#### Study limitations

This study covered only a small number of patients at a single-center study, so that future studies of larger patient populations are necessary to validate our findings. In addition, the precise reasons for the low values of GLS and relatively preserved diastolic function in both CS and DCM patients in this study are unknown. Although a small number of patients may effect on these findings, future studies of larger patient populations are also necessary to clarify. An important limitation of our study is that investigation of long-term clinical outcomes or follow-up data after medical therapy for patients with CS were not part of the study. One limitation of image acquisition for 3-D speckle-tracking is the relatively slow volume rate of 20–30 volumes/s. However, the reproducibility of the 3-D speckle-tracking system used in this study proved to be satisfactory. Another limitation was that none of patients had exercise stress echocardiographic data. These data might help to detect subclinical myocardial dysfunction and lead to more accurate prediction of CS patients. Finally, patients with diabetes mellitus included in CS (1 patients) and DCM (3 patients) groups in this study. The presence of diabetes mellitus may effect on LV myocardial function, especially associated with reduced longitudinal myocardial function. However, when patients with diabetes mellitus were excluded from analysis, the overall results were similar.

#### Conclusions

3-D speckle-tracking radial strain appears to be capable of differentiating CS from DCM among cases with relatively mild LV systolic dysfunction. These findings may well have clinical implications for the management of such patients.

**Conflict of interest** None.

#### References

1. Newman LS, Rose CS, Maier LA (1997) Sarcoidosis. *N Engl J Med* 336(17):1224–1234

2. Deng JC, Baughman RP, Lynch JP 3rd (2002) Cardiac involvement in sarcoidosis. *Semin Respir Crit Care Med* 23(6):513–527
3. Chiu CZ, Nakatani S, Zhang G, Tachibana T, Ohmori F, Yamagishi M, Kitakaze M, Tomoike H, Miyatake K (2005) Prevention of left ventricular remodeling by long-term corticosteroid therapy in patients with cardiac sarcoidosis. *Am J Cardiol* 95(1):143–146
4. Luk A, Metawee M, Ahn E, Gustafsson F, Ross H, Butany J (2009) Do clinical diagnoses correlate with pathological diagnoses in cardiac transplant patients? The importance of endomyocardial biopsy. *Can J Cardiol* 25(2):e48–e54
5. Nesser HJ, Mor-Avi V, Gorissen W, Weinert L, Steringer-Mascherbauer R, Niel J, Sugeng L, Lang RM (2009) Quantification of left ventricular volumes using three-dimensional echocardiographic speckle tracking: comparison with MRI. *Eur Heart J* 30(13):1565–1573
6. Tanaka H, Hara H, Adelstein EC, Schwartzman D, Saba S, Gorcsan J 3rd (2010) Comparative mechanical activation mapping of RV pacing to LBBB by 2D and 3D speckle tracking and association with response to resynchronization therapy. *JACC Cardiovasc Imaging* 3(5):461–471
7. Tanaka H, Hara H, Saba S, Gorcsan J 3rd (2010) Usefulness of three-dimensional speckle tracking strain to quantify dyssynchrony and the site of latest mechanical activation. *Am J Cardiol* 105(2):235–242
8. Thebault C, Donal E, Bernard A, Moreau O, Schnell F, Mabo P, Leclercq C (2011) Real-time three-dimensional speckle tracking echocardiography: a novel technique to quantify global left ventricular mechanical dyssynchrony. *Eur J Echocardiogr* 12(1):26–32
9. Soejima K, Yada H (2009) The work-up and management of patients with apparent or subclinical cardiac sarcoidosis: with emphasis on the associated heart rhythm abnormalities. *J Cardiovasc Electrophysiol* 20(5):578–583
10. Uemura A, Morimoto S, Hiramitsu S, Kato Y, Ito T, Hishida H (1999) Histologic diagnostic rate of cardiac sarcoidosis: evaluation of endomyocardial biopsies. *Am Heart J* 138(2 Pt 1):299–302
11. Fahy GJ, Marwick T, McCreery CJ, Quigley PJ, Maurer BJ (1996) Doppler echocardiographic detection of left ventricular diastolic dysfunction in patients with pulmonary sarcoidosis. *Chest* 109(1):62–66
12. Uemura A, Morimoto S, Kato Y, Hiramitsu S, Ohtsuki M, Kato S, Sugiura A, Miyagishima K, Iwase M, Hishida H (2005) Relationship between basal thinning of the interventricular septum and atrioventricular block in patients with cardiac sarcoidosis. *Sarcoidosis Vasc Diffuse Lung Dis* 22(1):63–65
13. Patel MR, Cawley PJ, Heitner JF, Klem I, Parker MA, Jaroudi WA, Meine TJ, White JB, Elliott MD, Kim HW, Judd RM, Kim RJ (2009) Detection of myocardial damage in patients with sarcoidosis. *Circulation* 120(20):1969–1977
14. Smedema JP, Snoep G, van Kroonenburgh MP, van Geuns RJ, Cheriex EC, Gorgels AP, Crijns HJ (2005) The additional value of gadolinium-enhanced MRI to standard assessment for cardiac involvement in patients with pulmonary sarcoidosis. *Chest* 128(3):1629–1637
15. Tadamura E, Yamamuro M, Kubo S, Kanao S, Saga T, Harada M, Ohba M, Hosokawa R, Kimura T, Kita T, Togashi K (2005) Effectiveness of delayed enhanced MRI for identification of cardiac sarcoidosis: comparison with radionuclide imaging. *AJR Am J Roentgenol* 185(1):110–115
16. Patel AR, Klein MR, Chandra S, Spencer KT, Decara JM, Lang RM, Burke MC, Garrity ER, Hogarth DK, Archer SL, Sweiss NJ, Beshai JF (2011) Myocardial damage in patients with sarcoidosis and preserved left ventricular systolic function: an observational study. *Eur J Heart Fail* 13(11):1231–1237
17. Seo Y, Ishizu T, Enomoto Y, Sugimori H, Yamamoto M, Machino T, Kawamura R, Aonuma K (2009) Validation of 3-dimensional speckle tracking imaging to quantify regional myocardial deformation. *Circ Cardiovasc Imaging* 2(6):451–459
18. Cheong BY, Muthupillai R, Nemeth M, Lambert B, Dees D, Huber S, Castriotta R, Flamm SD (2009) The utility of delayed-enhancement magnetic resonance imaging for identifying non-ischemic myocardial fibrosis in asymptomatic patients with biopsy-proven systemic sarcoidosis. *Sarcoidosis Vasc Diffuse Lung Dis* 26(1):39–46
19. Kim JS, Judson MA, Donnino R, Gold M, Cooper LT Jr, Prystowsky EN, Prystowsky S (2009) Cardiac sarcoidosis. *Am Heart J* 157(1):9–21
20. Remme WJ, Swedberg K (2002) Comprehensive guidelines for the diagnosis and treatment of chronic heart failure. Task force for the diagnosis and treatment of chronic heart failure of the European Society of Cardiology. *Eur J Heart Fail* 4(1):11–22
21. Ardehali H, Kasper EK, Baughman KL (2005) Diagnostic approach to the patient with cardiomyopathy: whom to biopsy. *Am Heart J* 149(1):7–12